Supporting Information for

Nanotexturing To Enhance Photoluminescent Response of Atomically Thin Indium Selenide with Highly Tunable Band Gap

Mauro Brotons-Gisbert[¶], *Daniel Andres-Penares*[¶], *Joonki Suh*[⊥], *Francisco Hidalgo*[§], *Rafael Abargues*[†], *Pedro J. Rodríguez-Cantó*[†], *Alfredo Segura*[¶], *Ana Cros*[¶], *Gerard Tobias*[‡], *Enric Canadell*[‡], *Pablo Ordejón*[§], *Junqiao Wu*[⊥], *Juan P. Martínez-Pastor*[¶,*], *Juan F. Sánchez-Royo*[¶,*]

[¶]ICMUV, Instituto de Ciencia de Materiales, Universidad de Valencia, P.O. Box 22085, 46071 Valencia, Spain

[⊥]Department of Materials Science and Engineering, University of California, Berkeley, California 94720, United States

[§]Catalan Institute of Nanoscience and Nanotechnology (ICN2), CSIC and The Barcelona Institute of Science and Technology, Campus UAB, Bellaterra, 08193 Barcelona, Spain,

[†]Intenanomat S.L., c/ Catedrático José Beltrán 2, 46980 Paterna, Spain

[‡]Institut de Ciència de Materials de Barcelona (ICMAB-CSIC), Campus de la UAB, 08193 Bellaterra, Barcelona, Spain

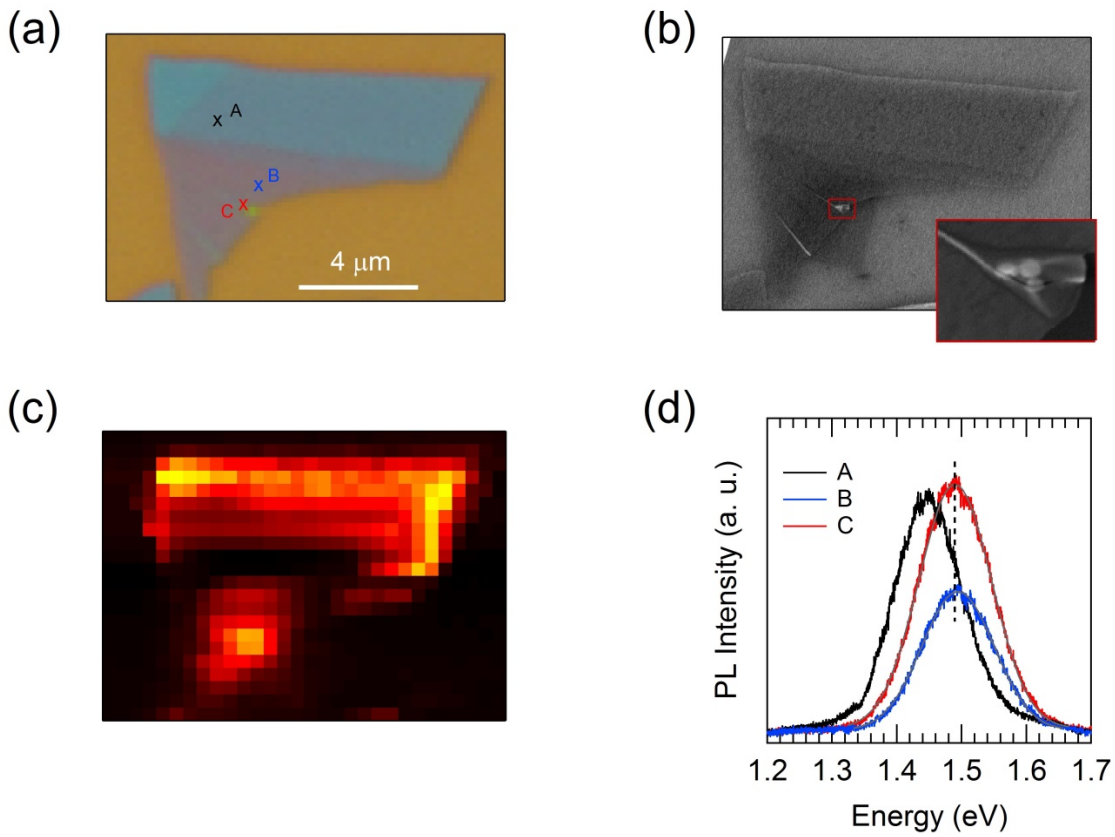

Figure S1. Few-layer InSe nanosheets lifted up by few SiO_2 nanoparticles. (a) Optical image of an InSe nanosheet with a thin and uniform terrace of 4 nm in thickness. This thin terrace shows some lifting due to the presence of few NPs trapped under it, which can be distinguished in the proximity of the labelled C-point. (b) SEM image of the nanosheet shown in Figure S1a. The SEM image at the inset is a detailed view of the region indicated by a red rectangle depicted on the main SEM image. (c) Integrated-PL intensity map measured in the InSe nanosheet of Figure S1a. The Integration was performed in the 1.2-1.7 eV range. (d) Micro-PL spectra acquired in selected points of the nanosheet, which correspond to those labeled from A to C in the optical image of the Figure S1a. The spectrum measured at the A point (with peak maximum at 1.442 ± 0.001 eV) comes from a 5 nm-thick nanosheet, whereas those measured at the B and C points come from a 4-nm thick nanosheet (with peak maximum at 1.490 ± 0.001 eV). The PL

intensity acquired in textured points of the 4-nm nanosheet (C-point) is enhanced by a factor ~2 with respect to that measured in its flatter part (B-point), becoming as intense as the PL signal acquired in a flat 5-nm thick nanosheet (A-point).

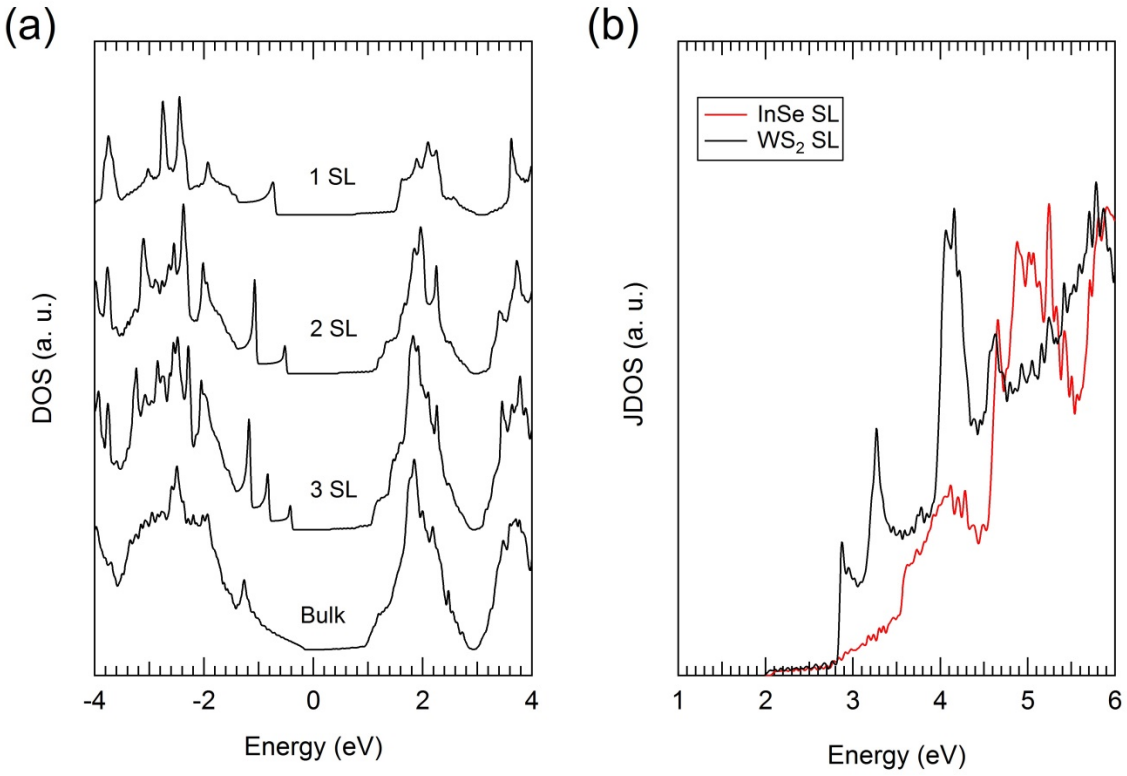

Figure S2. Electronic properties of 2D InSe nanosheets. (a) Density of states calculated for bulk InSe and 3, 2 and 1 SLs. Starting from the valence and conduction band edges, the density of states of the bulk exhibits the continuous ~$E^{1/2}$ dependence expected for delocalized bands, until more localized bands are reached (as the p_x-p_y valence band states observed at energies lower than -1 eV in bulk InSe). Quantum-size confinement effects introduce van Hove singularities in the density of states of atomically thin InSe nanosheets. (b) The joint density of states (JDOS) calculated for InSe SL, which has been shifted in energy by 0.9 eV to take into account the well-known underestimation of band gap values calculated by density functional theory. For ease of comparison, we also show the joint density of states calculated for WS_2 SL.

For energies below ~2.8 eV, i. e., most of the visible spectrum, the JDOS calculated for 2D InSe and WS_2 similarly exhibit a monotonous increase as energy increases. However, only for energies higher than 2.8 eV, the presence of strong van Hove singularities relatively enhances the density of available states for optical transitions in WS_2.[1]

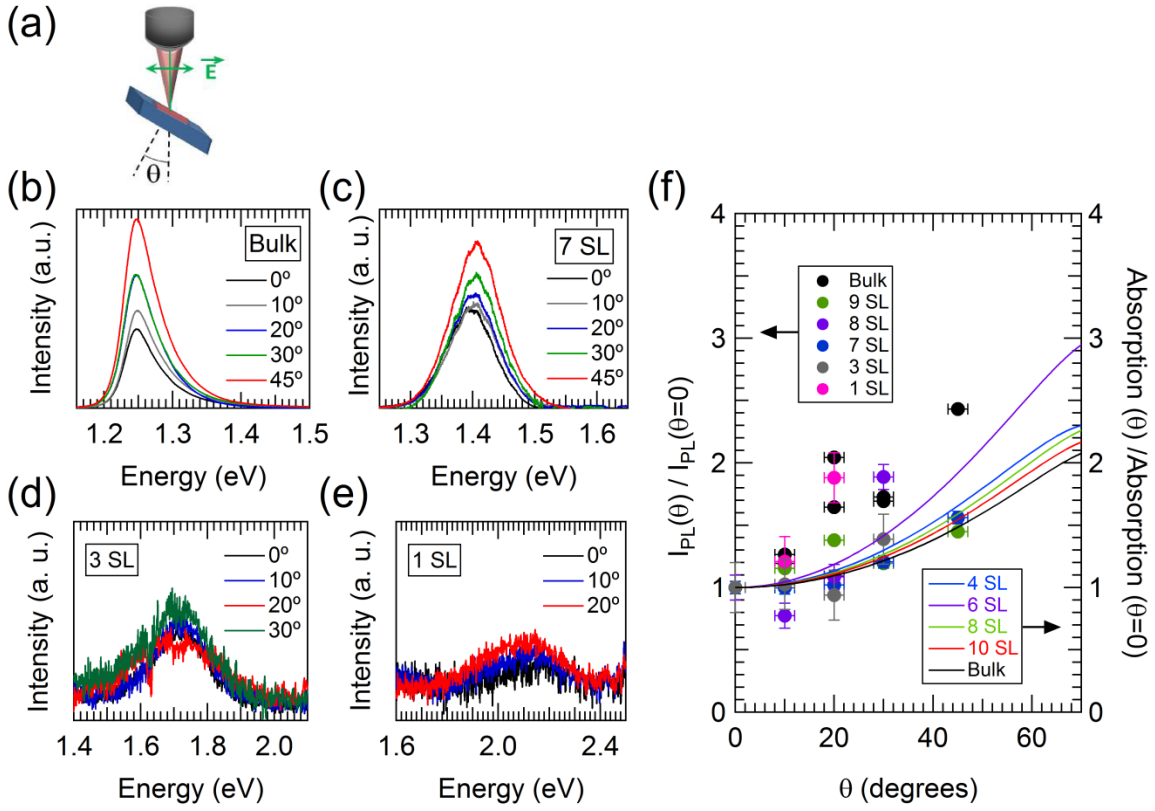

Figure S3. Angular dependence of the μ-PL in flat InSe nanosheets. (a) Illustration of the procedure to perform μ-PL measurements in flat InSe nanosheets as a function of the emission/collection angle θ. Notice that the polarization of the excitation light was placed perpendicular to the rotation axis. The excitation wavelength was 532 nm. (b)-(e) Micro-PL spectra collected in bulk and InSe nanosheets placed at different θ. The thickness of the nanosheets and the θ used for each acquisition are indicated on each plot. (f) Summary of the integrated μ-PL peak intensities obtained for each nanosheet at different θ positions. All the

intensity values obtained have been normalized to that obtained for θ=0 (left ordinate axis). The relative light absorption ratio has been included (right ordinate axis), as estimated by 1-exp[-α(θ)*d*(*θ*)] and normalized to its value obtained at θ=0, where *d*(*θ*)=*d*/*cos*(*θ*), $1/\alpha^2(\theta) = sin^2(\theta)/\alpha_{\parallel c}^2 + cos^2(\theta)/\alpha_{\perp c}^2$. The $\alpha_{\parallel,\perp c}$ have been estimated from the *Im ε*(*ω*) (Figure 3) at the excitation energy of 2.33 eV These results evidence the anisotropy of the optical properties of bulk InSe and nanosheets.

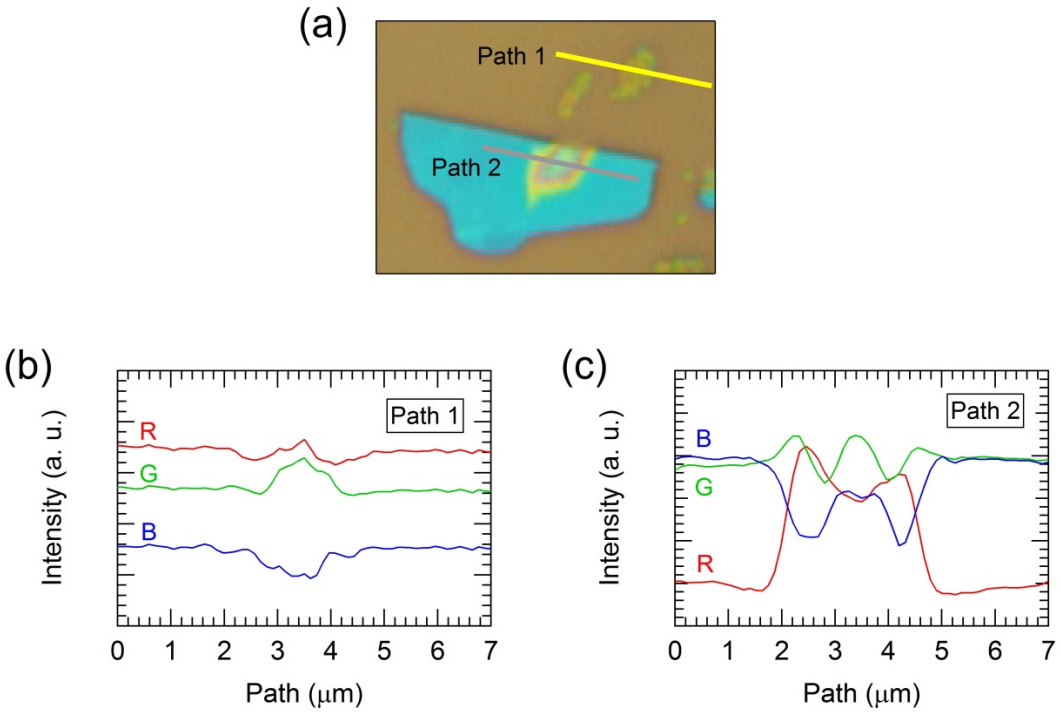

Figure S4. Light scattering by SiO_2 NPs. (a) Optical image of a 12-nm thick InSe nanosheet, which has been also shown in Figure 1b. On this image, we have marked two paths, one cross over non-covered SiO_2 NPs (Path 1) and one over the lifted region of the InSe nanosheet due to the presence of NP agglomerates (Path 2). The intensity of the R, G, and B channels has been extracted from the optical image of the nanosheet, along these two paths. (b) Intensity of the R, G, and B channels obtained along the Path 1. These curves reflect that, within the visible

spectrum, the used NPs act as effective light-scattering centers of red and green wavelengths. (c) Intensity of the R, G, and B channels obtained along the Path 2. These curves clearly reflect a relative enhancement of the R channel at the border of the lifted region of the nanosheet. These results indicate that the presence of the trapped NPs favors light absorption since they act as light scattering centers.